Predictive Roll, Handling and Ride Control of Vehicles via Active Suspensions

Qilun Zhu and Beshah Ayalew

Abstract—This paper focuses on the application of active suspensions to vehicles with solid-axles for medium and light duty trucks. These vehicles are prone to rollover issues and compromised ride quality. A cascade control structure is proposed considering a time scale analysis of the various modes in the vehicles' dynamics. The structure consists of: a) an upper level predictive anti-roll controller that uses road preview information for generating an optimal reference roll angle, yaw rate and roll moment distribution, and b) a lower level sprung/unsprung mass motion controller that tracks the reference roll angle and regulates other states. Simulation results indicate that the proposed system is able to reduce sprung mass acceleration, improve tire-road contact, stabilize roll motion and enhance the yaw response of the vehicle.

I. INTRODUCTION

In modern vehicles, ever-increasing customer expectations of safety, comfort, handling and ride quality demand a well-integrated suspension system design. To optimize for all these expectations, active suspension systems have been in development for the last few decades. However, due to cost reasons, most of the active suspension designs have been fully independent suspensions targeted for luxury vehicles. Medium to light duty trucks (e.g. pickup trucks) and off-road vehicles are often designed with dependent solid-axle suspensions. With fewer linkages and no CV joints, dependent suspensions offer better reliability and durability for the targeted functions of these vehicles. However, dependent solid-axle suspensions involve large unsprung masses and entail a dynamic coupling between the tire/wheel motions in the left and right corners. These factors, combined with the typically high CG position of these vehicles lead to poor ride quality, unsatisfactory handling performance, and high risk of rollover compared to luxury vehicles with independent suspensions. In addition, these vehicles are also very often used off-road, with variable loading, and feature much higher power to weight ratio, which increases their chances of being involved in high speed cornering events with poor road traction conditions. All these considerations make active dependent suspensions an attractive option for medium to light duty vehicles with off-road use.

Whether the suspension system is dependent or independent, the main objectives of incorporating active suspensions are rollover prevention, improving ride quality and enhancing handling performance. There are numerous previous research works about each of these topics. Since the 1970s, partially active suspensions (e.g. active anti-roll bars) have been applied to stabilize the roll motion of a vehicle's sprung mass [1][2][3][4]. Most of these applied linear 3DOF vehicle models (roll, yaw and slip) for simulation and controller design. Although ride quality and handling performance were not the main concerns with these approaches, the 3 DOF model provided analytical understanding of roll-yaw coupling and the possibility of integrating nonlinear tire behavior in the controller design.

Ride quality became the primary concern of active suspension systems with the development of high bandwidth independently actuated hydraulic units. Decoupling between the left and right actuators made it possible not only to stabilize roll motion but also the pitch and bounce motions of the sprung mass [5]. Based on the Multiple Input Multiple Output (MIMO) nature of this control problem, Linear Quadratic (LQ) controllers designed based on a full vehicle model were proposed by many authors [6][7]. More recently, ref [8] discussed the possibility of applying Model Predictive Control (MPC) to reduce actuation effort, improve ride quality and stabilize vertical tire loads. In their work, road surface disturbance is previewed using an optical terrain scan and the control problem is posed as one of minimizing both control effort and sprung mass acceleration for a future prediction horizon. The present work is in part inspired by the road preview use in ref [8], but it goes beyond just ride quality.

Many works considered the possibility of improving handling performance with active suspensions [9][10][11][12]. These works manipulated lateral load transfer via front/rear Roll Moment Distribution (RMD) to influence cornering stiffness distributions and thereby the lateral dynamics, assuming that roll motion is easily stabilized. These strategies neglect that fact that under some transient scenarios an active suspension could be made to intentionally increase roll angle inward or outward using say, previewed road curvature, to reduce actuation effort and improve handling stability. On the other hand, for comfort considerations, the roll angle of the sprung mass should be as small as possible. Combining these considerations leads to a MIMO optimal control problem. However, RMD affects yaw rate and slip angle nonlinearly [9]–[13], which causes many practical issues for implementing online optimal controllers. The present paper provides an intuitive analysis of these nonlinear characteristics of RMD and how they may be accommodated with a scheduled linearization and online quadratic optimization.

It turns out that the above three objectives can be met with a control structure that exploits the time scale separation

Q. Zhu and B. Ayalew are with the Clemson University-International Center for Automotive Research, Greenville, SC, 29607 (Corresponding author: qilun@g.clemson.edu; beshah@clemson.edu, Phone: 864-283-7228, Fax: 864-283-7208).

between unsprung mass dynamics, sprung mass dynamics and driver steer input. A hierarchical or cascade structure that separates the coupled system dynamics into a slow upper level control layer and fast lower level control layer has been applied in many control projects [14][15]. The advantage of this methodology is that it reduces the model order for the upper level controller by assigning the task of managing the high frequency dynamic modes to the lower level controller. Therefore, the upper level controller has more execution time to run more complex control algorithms and possibly generate reference/target signals for the lower level control loop to track. However, the interface between the two layers should be explicitly addressed. In the present paper, such an approach is proposed for control of a vehicle with active suspensions. In the cascade, a fast lower level LQG controller is used to improve ride quality and tire contact conditions, while the yaw rate response and roll stability is enhanced with a slower upper level MPC controller.

An additional feature incorporated in the proposed upper level MPC controller is the use of trajectory preview information. The idea of preview information has been used extensively in unmanned ground vehicle trajectory optimization [16] and for other advanced driver assist systems [17]. The approach we take here, however, targets reducing/optimizing the required RMD actuation effort while generating an optimal reference roll angle using the preview information.

The rest of the paper is organized as follows. Section II describes the vehicle model and control hierarchy. Section III gives the details of the upper-level control, including the predictive control formulation. Section IV details the lower-level sprung/unsprung mass motion control. Section V discusses select simulation results, followed by the conclusions of the work in Section VI.

II. VEHICLE MODEL AND CONTROL HIERARCHY

We adopt a 9 DOF full vehicle model for a vehicle with dependent solid axle suspensions(Figure 1) The equations describing this system can be derived via Lagrange's method. The 9 DOF $[v, r, z_s, \phi_s, \theta, z_{uf}, z_{ur}, \phi_{uf}, \phi_{ur}]$ along with the time derivatives of the last 7 DOF result in a 16th order nonlinear system. The reader is referred to the nomenclature for definitions of the symbols used.

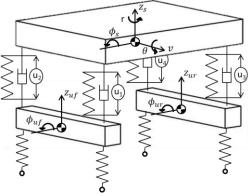
Figure 1: 9 DOF full vehicle model

We also adopt the empirical tire model [9][11] for the tire lateral force:

$$F_{tire} = C_1 \alpha F_z + C_2 \alpha F_z^2 \tag{1}$$

Including body roll to the "bicycle model" for handling, the relevant equations of motion are:

$$m(\dot{v} + Vr) + m_s h \ddot{\phi}_s = \sum F_{tire} \tag{2}$$

$$I_{zz}\dot{r} - I_{xz}\ddot{\phi}_s = a \sum F_{tire_f} - b \sum F_{tire\_r} \tag{3}$$

For a driver model, we shall use a simple controller with trajectory deviation feedback with first order lag:

$$\frac{\delta(s)}{D_e(s)} = \frac{K_d}{1 + \tau s} \tag{4}$$

where the deviation D_e is measured at predictive distance L_a ahead of the current position of the vehicle:

$$D_e = Y + \psi L_a - Y_L \tag{5}$$

A linearized eigen frequency analysis of the system (Table I) shows a clear time scale separation which suggests the suitability of a cascaded control structure, separating control tasks between the fast (unsprung mass) and slow (sprung mass) motions.

TABLE I: EIGEN FREQUENCY RANGES OF THE DIFFERENT MODES OF MOTION

Driver, yaw rate and slip	0.7-1.2 Hz
Roll, pitch and bounce	1.6 – 2.5 Hz
Unsprung mass dynamics	10 – 17 Hz

Figure 2 shows the proposed cascade control structure for the vehicle with an active suspension system. At the upper level, a model predictive control (MPC) framework is implemented to optimize between roll angle, yaw rate and actuation power. A practical consideration for adopting MPC for the upper level control is that there is enough time for online optimization in MPC since the eigen frequencies attributed to the handling modes (roll, yaw, slip) are slow.

The MPC control is provided with a future yaw rate reference and possibly future steering angle generated by the yaw rate prediction block (Figure 2). This prediction block executes an online closed-loop simulation of the driver model controlling a reference bicycle vehicle model to track the future/previewed trajectory reference (Y_{ref}). At the lower level, an LQG controller is designed focusing on controlling primarily the unsprung mass motion and but also tracking the sprung mass roll angle reference generated by the upper level MPC loop. This later aspect is necessary because, with the preview information, the MPC optimization may intentionally alter the reference roll angle to improve the vehicle's yaw response under transient scenarios. Vehicle modes considered in the lower loop have higher natural frequencies, which favor offline calibration of the LQG controller using standard design tools.
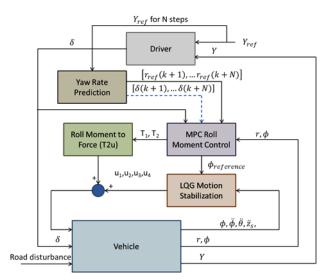
Figure 2: Cascade control of vehicle with active suspension system

III. UPPER LEVEL ANTI-ROLL MOMENT CONTROL

The actuation bandwidth is selected as 3 Hz according to the eigen frequency analysis (Table I). This excludes consideration of the unsprung mass dynamics, whose motions are assumed to be regulated with the low level LQG loop. Therefore, for the MPC design, the vehicle model is simplified to the 3 DOF one comprising of equations (2), (3) and (6).

$$I_{xx}\ddot{\phi}_s - I_{xz}\dot{r} - m_s h_s(\dot{v} + Vr) = \\ m_s h_s g\phi - (k_{\phi f}\phi + c_{\phi f}\dot{\phi}) - (k_{\phi r}\phi + c_{\phi r}\dot{\phi}) + T_1 + T_2 \quad (6)$$

This 3DOF model shows linear coupling between the yaw rate and roll angle states. However, the effect of the Roll Moment Distribution (RMD) is still not explicitly expressed. Assuming that the active suspension stabilizes the sprung mass roll motion ideally, $\phi_s = \dot{\phi}_s = \ddot{\phi}_s \equiv 0$, the 3 DOF model can be reduced to the 2 DOF model:

$$m(\dot{v} + Vr) = \sum F_{tire} \quad (7)$$

$$(I_{zz} + I_{xz})\dot{r} = \\ \left(\frac{m_s h_s}{m} + a\right)\sum F_{tire\_f} - \left(\frac{m_s h_s}{m} + b\right)\sum F_{tire\_r} + T_1 + T_2 \quad (8)$$

The front and rear wheel loads relate to the added roll moments according to:

$$F_{zf} = mg\frac{b}{W} \pm \frac{T_1}{L_1}; \quad F_{zr} = mg\frac{a}{W} \pm \frac{T_2}{L_2} \quad (9)$$

Substituting (9) into (1), (7) and (8), we have:

$$\dot{v} = \\ \frac{2}{m}\left[(C_{1f}W_f + C_{2f}W_f^2)\alpha_f + (C_{1r}W_r + C_{2r}W_r^2)\alpha_r \\ + C_{2f}\alpha_f\frac{T_1^2}{L_1^2} + C_{2r}\alpha_r\frac{T_2^2}{L_2^2}\right] - Vr \quad (10)$$

$$\dot{r} = \\ \frac{2}{(I_{zz} + I_{xz})}\left[\left(\frac{m_s h_s}{m} + a\right)(C_{1f}W_f + C_{2f}W_f^2)\alpha_f \\ - \left(\frac{m_s h_s}{m} + b\right)(C_{1r}W_r + C_{2r}W_r^2)\alpha_r + \frac{1}{2}(T_1 + T_2) \\ + \left(\frac{m_s h_s}{m} + a\right)C_{2f}\alpha_f\frac{T_1^2}{L_1^2} - \left(\frac{m_s h_s}{m} + b\right)C_{2r}\alpha_r\frac{T_2^2}{L_2^2}\right] \quad (11)$$

where, the front and rear axle slip angles are given by:

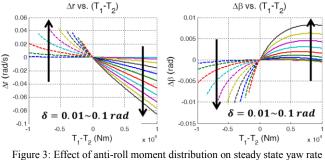$$\alpha_f = \frac{v+ra}{V} - \delta; \quad \alpha_r = \frac{v-rb}{V}$$

Equation (10) and (11) indicate that the RMD (= $(T_1 - T_2)$) affects handling performance nonlinearly. A similar conclusion is also drawn in [9] using a different approach. This point is illustrated further in Figure 3, which show the steady state Δr and $\Delta\beta$ responses (from β and r values at $T_1 - T_2$=0) versus the RMD for different steer angles δ. These two figures indicate that roll moment distribution has a large influence on β and r. The use of a linearized model seems acceptable. However, it can also be observed that control authority of the roll moment distribution over yaw rate and body slip angle is greatly influenced by the prevailing steer angle. This suggests scheduling the linearization with respect to steer angle (in addition to vehicle speed, as we do below).

We derive a nonlinear MPC (or nMPC) design as follows. The vehicle speed is assumed to be constant during the maneuver and the 3 DOF vehicle model can be written in the following nonlinear state space form:

$$\dot{x}_{MPC} = A_{MPC}(\delta, V)x_{MPC} + B_{MPC}(\delta, V)u_{MPC} \\ y_{MPC} = C_{MPC}x_{MPC} \quad (12)$$

where:

$$x_{MPC} = [r, v, \phi_s, \dot{\phi}_s]^T; \quad y_{MPC} = [r, \phi_s]^T; \\ u_{MPC} = [T_1, T_2]^T$$

Figure 3: Effect of anti-roll moment distribution on steady state yaw rate response at 90 km/h.

Discretizing this above model at a chosen sampling interval (here 0.1s), we obtain:

$$x_{MPC}(k + 1) = \\ A_d(\delta(k), V)x_{MPC}(k) + B_d(\delta(k), V)u_{MPC}(k) \quad (13)$$

$$y_{MPC}(k) = C_d x_{MPC}(k)$$

Prediction of the output for future horizon N can be done by:

$$Y_{N+1} = F_N X_0 + G_N U_N \quad (14)$$

where:

$Y_{N+1} = [y_{MPC}(k+1), \cdots y_{MPC}(k+N)]^T$;

$X_0 = [x_{MPC}(k), u_{MPC}(k)]^T$;

$U_N = [u_{MPC}(k+1), \cdots u_{MPC}(k+N)]^T$

As mentioned before, given future trajectory information, the future steering input sequence $\delta(k+1) \ldots \delta(k+N)$ can be estimated from the yaw rate prediction block (Figure 2). For the N-step prediction horizon at time k, F_N and G_N are constant matrices. A practical methodology to simplify the formulation of (13) is to assume the system to be linear time invariant for the prediction horizon. Then:

$$F_N = \begin{bmatrix} C_d A_d^2(\delta(k)) & C_d A_d(\delta(k))B_d(\delta(k)) \\ \vdots & \vdots \\ C_d A_d^{N+1}(\delta(k)) & C_d A_d^N(\delta(k))B_d(\delta(k)) \end{bmatrix}$$
$$G_N = \begin{bmatrix} C_d B_d(\delta(k)) & \cdots & 0 \\ \vdots & \ddots & \vdots \\ C_d A_d^{N-1}(\delta(k))B(\delta(k)) & \cdots & C_d B_d(\delta(k)) \end{bmatrix} \quad (15)$$

The drawback of this simplification is that future steering angles are not included. However, for a short prediction horizon and a reasonable MPC updated rate, with new driver steering angles at each MPC update, acceptable results can be obtained. Recall that the vehicle system model linearization is still scheduled with respect to steer angle per the analysis depicted in Figure 3. Furthermore, the future predicted yaw rate reference is still included in the MPC optimization as discussed below.

The optimal control sequence for prediction horizon N can be solved for using quadratic programming. The optimization problem is posed as follows:

$$\min[(Y_{N+1}(\delta) - R_{NN})^T Q_y(\delta)(Y_{N+1}(\delta) - R_{NN})$$
$$+ U_N^T P_u U_N] \quad (16)$$
$$s.t.\ LB_u < U_N < UB_u$$
$$LB_y < Y_{N+1} < UB_y$$

where:
$$R_{NN} = \left[[r_{ref}(k+1), \phi_{ref}(k+1)], \cdots [r_{ref}(k+N), \phi_{ref}(k+N)] \right]^T$$

r_{ref} is the reference yaw rate sequence from the yaw rate prediction block (Figure 2); ϕ_{ref} is the reference roll angle input for the MPC block and it is set as zero. Note that this is different from $\phi_{reference}$ in Figure 2. Q_y and P_u are the weighting matrices of reference tracking performance and control effort.

Substituting (14) into (16):
$$\min[(F_N X_0 + G_N U_N - R_{NN})^T Q_y(\delta)(F_N X_0 + G_N U_N$$
$$- R_{NN}) + U_N^T P_u U_N]$$
$$s.t.\ LB_u < U_N < UB_u \quad (17)$$

$$G_N^{-1}(LB_y - F_N X_0) < U_N < G_N^{-1}(UB_y - F_N X_0)$$

The lower bound and upper bound of the control effort (LB_u and UB_u) are selected according to available actuator capacity. Constraints of yaw rate and roll angle can be calculated based on friction coefficient and suspension travel (rattle space).

For the MPC implementation in this work, a prediction horizon of 2 seconds and an MPC update rate of 0.1 seconds have been used. The former is of the order of 50m preview distance at a vehicle speed of 90km/hr.

IV. LOWER LEVEL MOTION CONTROL

For vehicles with dependent suspensions, the usually large unsprung inertia influence body acceleration magnitudes in high frequency range. The required minimum bandwidth of actuation for controlling both sprung and unsprung mass motions is then about 20 Hz. Assuming that this is achievable, a MIMO LQG motion controller can be designed as follows. Since yaw rate and slip angle are not evaluated in the LQG loop, the system model can be reduced to a 7 DOF model. Roll angle reference is passed down as an output of the MPC optimization loop. Equation (19) describes the closed-loop dynamics of the lower level control loop.

$$\begin{bmatrix} \dot{x}_{7DOF} \\ \dot{\tilde{x}} \end{bmatrix} =$$
$$\begin{bmatrix} A_{7DOF} & -B_{7DOF}u_{LQG}F \\ L_{LQG}C_y & A_{7DOF} - B_{7DOF}u_{LQG}F - L_{LQG}C_y \end{bmatrix} \begin{bmatrix} x_{7DOF} \\ \tilde{x} \end{bmatrix}$$
$$+ \begin{bmatrix} B_w \\ 0 \end{bmatrix} w + \begin{bmatrix} 0 \\ L_{LQG} \end{bmatrix} v + \begin{bmatrix} 0 \\ -L_{LQG} \end{bmatrix} r_y \quad (19)$$

$$\hat{y} = C\hat{x}$$

where:
$\tilde{x}$: states of estimator ; $y_{LQG} = [\phi, \dot{\phi}, \dot{\theta}, \dot{z}_s]^T$;
$r_y = [\phi_{MPC}, 0,0,0]^T$; $u = [u_1, u_2, u_3, u_4]^T$;
F: optimal control gain from LQR.
L_{LQG}: optimal estimation gain from Kalman filter

V. SIMULATION RESULTS

Simulations are conducted with the proposed active suspension control system implemented on a vehicle with dependent suspensions and the following main parameters.

TABLE II: MAIN PARAMETERS OF THE VEHICLE USED FOR SIMULATION

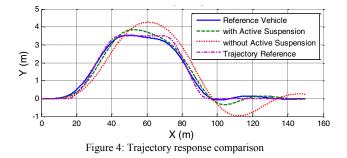| Vehicle Type	Pickup truck
Vehicle mass	2298 kg
Unsprung mass	150 kg (front) 150 kg (rear)
Static weight distribution	63/37 (front/rear)
Wheel base × track width	4 m×2 m
Suspension spring rate	198 kN/m (front) 300 kN/m (rear)
Suspension damping	5000 N/(m/s) (front & rear)
Tire vertical spring rate	250 kN/m

The proposed cascade active suspension control is evaluated in simulations of a 90 km/h Double Lane Change (DLC) maneuver. The power spectral density of the road

surface elevation is set as 5×10^{-6} m²/Hz. The reference vehicle is simply a bicycle model with the same mass and wheelbase as the truck. However, the weight distribution is 55/45, which results in close to a neutral steer (considered ideal) handling tendency.

As can be seen in Figure 4, the active suspension system reduces the understeer tendency of the original vehicle without inducing any instability. As the result, the trajectory tracking performance is significantly improved. The active suspension system also reduces roll angle and improves yaw response as expected (Figure 5). There are some transient scenarios (around 1.5s and 3.5s) where the roll angle is intentionally increased to improve yaw response due to the preview information incorporated in the MPC optimization. In some other cases (around 0.3s and 4.5s), an opposing roll motion is initiated just before the actual steer maneuver. This action increases the roll stability of the vehicle and saves peak actuation effort.

Figure 6 indicates that actuation of MPC is significantly slower and of higher magnitude than the LQG actuation (This comparison is after converting to same units with the distance between left and right actuators at 1.2 m). This observation supports the approach we took to apply Kalman Filtering in the MPC loop, which treated the LQG output as a disturbance. In addition, this difference in the nature of the required actuation effort for the two control loops suggests that two different sets of actuation devices may have to be used (or a multi-bandwidth peak force device must be constructed). Some solutions already exist on the market (e.g.[5]).

It can be observed from Figure 6 (top) that long prediction horizon (N=20) contributes to reduce the actuation effort. This possibility of optimizing actuation effort may not be possible from merely feedback (without preview/ predictive) control schemes.

Figure 4: Trajectory response comparison

In addition to improving the yaw responsiveness, and reducing low frequency sprung mass accelerations of the pickup truck, a specific advantage of applying active control on dependent solid-axle suspension can be observed from Figure 7. The magnitude response of one wheel to the disturbance applied at the other three wheels is significantly reduced. In other words, the proposed control scheme for the active suspension system serves to effectively remove the cross-coupling that existed (without the active suspension) between the corners, leading to improved tire-road contact

condition and ride quality (20 dB reduction of body acceleration within 0-20 Hz).
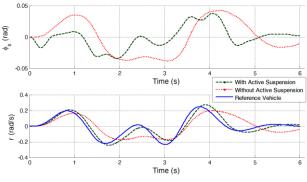

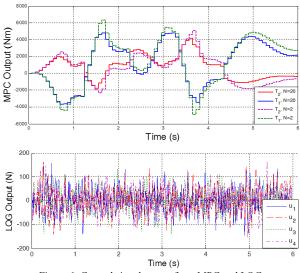
Figure 5: Roll angle and yaw rate performance

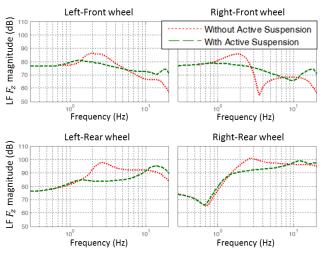
Figure 6: Control signal output from MPC and LQG.

Figure 7: Frequency response of left-front tire vertical load to road surface input on all four wheels.

VI. Conclusion

In this paper, a cascade control structure has been proposed for a fully active suspension for a vehicle with solid axles. The low bandwidth upper level MPC controller utilizes trajectory preview information to reduce roll motion, improve yaw rate response and optimize the front/ rear anti-roll moment distribution. The high bandwidth lower level LQG controller reduces sprung mass pitch and bounce motion. It also improves tire-road contact conditions by stabilizing unsprung mass dynamics. Some of the additional observations include: 1) as postulated, preview information can be used to positively influence peak actuation efforts including steer angles by essentially pre-determining the desired vehicle roll angle, 2) the cascade design results in actuator efforts that feature separate bandwidth/magnitude requirements for the two control levels, and 3) the proposed approach suppresses cross-coupling between corners in a solid-axle suspension in the difficult to manage wheel-hop frequency regimes.

Appendices

A. Nomenclature

v	Lateral velocity
r	Yaw rate
V	Forward speed
z_s, z_{uf}, z_{ur}	Vertical displacement (sprung mass, front unsprung mass , rear unsprung mass)
$\phi_s, \phi_{uf}, \phi_{ur}$	Roll angle (sprung mass, front unsprung mass , rear unsprung mass)
θ	Pitch angle
F_{tire}	Tire lateral force
C_1, C_2	Tire cornering stiffness coefficients
α	Tire slip angle
m, m_s	Mass (vehicle, sprung mass)
h_s	Height of sprung mass CG from plane defined by contact points of suspension springs and sprung mass.
$I_{xx}, I_{xz}, I_{yy}, I_{zz}$	Moments of inertia of sprung mass
a, b	Distance from front/rear axle to CG
δ	Steer angle
D_e	Deviation from reference trajectory
K_d	Driver proportional gain
τ	Driver response time constant
Y, Y_L	Vehicle lateral position, reference lateral position
ψ	Yaw angle
L_a	Driver predictive distance
u_1, u_2, u_3, u_4	Force generated by hydraulic units
T_1, T_2	Anti-roll moment from MPC
$k_{\phi f}, k_{\phi r}$	Sprung mass roll stiffness
$c_{\phi f}, c_{\phi r}$	Sprung mass roll damping
W	Wheelbase
L_1, L_2	Distance between left and right actuator (front/rear)
A, B, C, D	State space matrices
LB, UB	Lower and upper bounds
$*_f, *_r$	Notation of front and rear

References

[1] H. Yu, L. Güvenç, and Ü. Özgüner, "Heavy duty vehicle rollover detection and active roll control", *Vehicle system Dynamics: International Journal of Vehicle Mechanics and Mobility*, vol. 46, no. 6, pp. 451–470, Jun. 2008.

[2] A.T. Pham, and P. Ugazio, "Basic developments of an active air suspension for passengers cars", *SAE Technical Paper* 890095, pp.175–181 1989.

[3] N. Zulkarnain, F. Imaduddin, H. Zamzuri, and S.A. Mazlan, "Application of an active anti-roll bar system for enhancing vehicle ride and handling", in *Proc. the 2012 IEEE Colloquium on Humanities, Science & Engineering Research*, Dec. 2012, pp. 260–265

[4] D.J.M. Sampson, "Active Roll Control of Articulated Heavy Vehicles", Ph.D. dissertation, Dept. of Eng.., University of Cambridge, Cambridge, UK, 2000, pp.79–111.

[5] B.L.J. Gysen, J.J.H. Paulides, J.L.G. Janssen, and E.A. Lomonova, "Active electromagnetic suspension system for improved vehicle dynamics", *IEEE Transactions on Vehicular Technology*, vol.59, no. 3, pp. 1156–1163, Mar. 2010.

[6] R.Darus, and Y.M. Sam, "Modeling and control active suspension system for a full car model", in *Proc. 2009 5th International Colloquium on Signal Processing & Its Applications*, 2009, pp.13–18.

[7] S.H. Zareh, A. Sarrafan, A.F. Jahromi, and A.A. Khayyat, "Linear quadratic Gaussian application and clipped optimal algorithm using for semi active vibration of passenger car", in *Proc. 2011 IEEE International Conference on Mechatronics*, Apr. 2011, pp. 122–27.

[8] C. Gohrle, A. Wagner, A. Schindler, and O. Sawodny, "Active suspension controller using MPC based on a full-car model with preview information", in *Proc. 2012 American Control Conference*, Jun. 2012, pp. 497–502.

[9] D.E. Williams, and W.M. Haddad, "Nonlinear control of roll moment distribution to influence vehicle yaw characteristics", *IEEE Transactions on Control Systems Technology*, vol. 3, no. 1, pp.110–116, Mar. 1995.

[10] M. Lakehal–Ayat, S. Diop and E. Fenaux, "An improved active suspension yaw rate control", in *Proc. 2002 American Control Conference*, May. 2002, vol. 2, pp. 863–868.

[11] J. Wang, D.A. Wilson, W. Xu, and D.A. Crolla, "Active suspension control to improve vehicle ride and steady-state handling", in *Proc. 44th IEEE Conference on Decision and Control, and the European Control Conference*, Dec. 2005, pp. 1982–1987.

[12] M. Abe, "Study on effects of roll moment distribution control in active suspension on improvement of limit performance of vehicle handling", *International Journal of Vehicle Design*, vol. 15, no. 3–5, pp. 326–336, 1994.

[13] T.D. Gillispie, *Fundamentals of vehicle dynamics*, Warrendale, PA, Society of Automotive Engineers, Inc., 1992, pp. 209–217.

[14] C.M. Ying, S. Voorakaranam, and B. Joseph, "Analysis and performance of the LP-MPC and QP-MPC cascade control system", in *Proc. 1998 American Control Conference*, Jun. 1998, vol. 2, pp.806–810.

[15] G.V. Raffo, G.K. Gomes, J.E. Normey-Rico, C.R. Kelber, and L.B. Becker, "A predictive controller for autonomous vehicle path tracking", *IEEE Transaction on Intelligent Transportation System*, vol. 10, no. 1, pp. 92–102, Mar. 2009.

[16] J. Hardy, and M. Campbell, "Contingency planning over probabilistic hybrid obstacle predictions for autonomous road vehicles", in *Proc. 2010 International Conference on Intelligent Robots and Systems*, Oct. 2010, pp. 2237–2242

[17] C. Otto, and F.P. Leon, "Long–term trajectory classification and prediction of commercial vehicles for the application in advanced driver assistance systems", in *Proc. 2012 American Control Conference*, Jun. 2012, pp. 2904–2909.